

# A low-dimensional crystal growth model on an isotropic and quasi-free sustained substrate\*

Chenxi Lu(卢晨曦)<sup>1</sup>, Senjiang Yu(余森江)<sup>1</sup>, Lingwei Li(李领伟)<sup>1,†</sup>, Bo Yang(杨波)<sup>2</sup>,  
Xiangming Tao(陶向明)<sup>2</sup>, and Gaoxiang Ye(叶高翔)<sup>2,‡</sup>

<sup>1</sup>College of Materials and Environmental Engineering, Hangzhou Dianzi University, Hangzhou 310018, China

<sup>2</sup>Department of Physics, Zhejiang University, Hangzhou 310027, China

(Received 21 November 2019; revised manuscript received 3 January 2020; accepted manuscript online 9 January 2020)

A new crystal growth theoretical model is established for the low-dimensional nanocrystals on an isotropic and quasi-free sustained substrate. The driven mechanism of the model is based on the competitive growth among the preferential growth directions of the crystals possessing anisotropic crystal structures, such as the hexagonal close-packed and wurtzite structures. The calculation results are in good agreement with the experimental findings in the growth process of the low-dimensional Zn nanocrystals on silicone oil surfaces. Our model shows a growth mechanism of various low-dimensional crystals on/in the isotropic substrates.

**Keywords:** crystal growth, low-dimensional nanocrystals, isotropic substrates, preferential growth

**PACS:** 81.10.Aj, 81.07.Bc, 68.03.-g, 68.55.A-

**DOI:** 10.1088/1674-1056/ab6968

## 1. Introduction

Low-dimensional nanocrystals, including nanowires, nanorods, nanobelts, nanoplates, and nanosheets, etc., have triggered numerous fundamental and technological studies for their unique properties in recent decades.<sup>[1-3]</sup> Using them as active components, various types of nanoscale devices have been fabricated, such as photovoltaic,<sup>[4]</sup> thermoelectric,<sup>[5]</sup> and electromechanical<sup>[6]</sup> devices. The controllable growth of the low-dimensional nanocrystals in terms of the morphologies, sizes and microstructures is urgently desired for their practical applications.

These requirements have led to a rapidly evolving research on the preparation methods and growth mechanisms of the low-dimensional nanocrystals. To our knowledge, vapor deposition including physical vapor deposition (PVD) and chemical vapor deposition (CVD) is one of the most widespread methods for preparing the low-dimensional nanocrystals. Most of the vapor growth processes are based on solid substrates and dominated by the vapor-solid (VS)<sup>[2]</sup> or vapor-liquid-solid (VLS)<sup>[7]</sup> mechanism.

For the VS process, the one- or two-dimensional nanocrystals may be controllably fabricated on the well-designed substrates with specific patterns or crystal structures acting as templates.<sup>[3,8,9]</sup> However, the removal of the templates may damage the morphologies and microstructures of the nanocrystals. The well-known VLS growth method uses metal nanoparticles that form low-melting point eutectic alloys with the targeted materials to serve as the catalytic seeds

for the one- or two-dimensional crystal growth.<sup>[7,10]</sup> Except for the VS growth, the VLS and its variants, such as the vapor-solid-solid (VSS)<sup>[11]</sup> growth, require the use of suitable catalysts.

Recently, we reported the growth of various low-dimensional zinc (Zn) nanocrystals (for instance, nanowires, nanorods, nanobelts and nanoplates) with two main preferential growth directions of the [0001] and [01 $\bar{1}$ 0] directions on silicone oil surface by thermal evaporation, which is catalyst-free and achieved at room temperature.<sup>[12,13]</sup> Obviously, this phenomenon can not be explained by the VS and VLS mechanism. It is suggested that the growth of the low-dimensional Zn nanocrystals on the silicone oil surface should be related to the principle of minimum surface energy of the system.<sup>[14]</sup>

According to the theory proposed by Bravais and later modified by Donnay and Harker,<sup>[15]</sup> the crystal microstructure and morphology are closely related to its intrinsic crystal structure. In this case, the growth rates of the crystal planes are reversely proportional to the reticular densities, i.e., the number of lattice points per unit surface. In other words, there is a growth priority among the crystal planes corresponding to different growth directions, which results in a competitive growth where the crystal planes along the preferential growth directions overgrow the others.

Previous researches showed that the anisotropic crystal structures, such as the hexagonal close-packed (Zn, Be, Mg, Cd, Ti, etc.) and wurtzite (ZnO, ZnS, CdS etc.) structures, usually possess preferential growth directions owing to the

\*Project supported by the National Natural Science Foundation of China (Grant Nos. 11374082 and 51671048) and the Ten Thousand Talents Plan of Zhejiang Province of China (Grant No. 2018R52003).

†Corresponding author. E-mail: [lingwei@epm.neu.edu.cn](mailto:lingwei@epm.neu.edu.cn)

‡Corresponding author. E-mail: [gxye@zju.edu.cn](mailto:gxye@zju.edu.cn)

asymmetry of these crystal structures.<sup>[16–18]</sup> To be more exact, a crystal system with relatively less symmetry operations exhibits a stronger preferential growth tendency. For example, compared with those of the hexagonal close-packed and wurtzite structure, the characteristics of preferential growth directions of the face center cubic and zincblende structure are weaker due to their higher symmetry.

On the other hand, the liquid surface can be considered as an isotropic and quasi-free sustained substrate, where the deposition atoms diffuse randomly and freely.<sup>[19,20]</sup> The mean square displacement of the deposition atoms is given by  $\langle \Delta r^2 \rangle = 4D\Delta t$ , where  $D$  is the diffusion coefficient and  $\Delta t$  is the diffusion time.<sup>[21–23]</sup> The deposition atoms exhibit larger diffusion coefficients on the liquid surfaces than those on the solid substrates at room temperature.<sup>[19]</sup> Generally, the atomic diffusion and the growth of nanocrystals on the epitaxial interfaces are strictly guided by the crystal structures of the substrate surfaces. However, there is no need for the nanocrystals grown on the liquid substrate to match the microstructures of the amorphous isotropic liquid surface. The liquid surface effects mentioned above may highlight the characteristics of intrinsic preferential growth directions.

In this paper, we establish a new low-dimensional crystal growth model on the isotropic and quasi-free sustained substrate. The low-dimensional crystal growth does not depend on templates and catalysts, but is driven by the competitive growth among the preferential growth directions of the crystals with anisotropic crystal structures. The model gives a good explanation for the growth process of the low-dimensional Zn nanocrystals on the silicone oil surface. Furthermore, the model indicates the possibility to prepare various low-dimensional crystals on/in the isotropic substrates.

## 2. Model description

We suppose that atoms are deposited on an isotropic and quasi-free sustained substrate with constant flux  $f$ . The low-dimensional crystal growth model is described as follows:

(1) The deposition atoms diffuse freely and randomly on the substrate, then they nucleate and form seed crystals. The morphology of each seed crystal is a cuboid with sizes of  $l_0 \times w_0 \times h$ , where  $l_0$  and  $w_0$  are the initial length and width, respectively, and the height  $h$  is assumed to be a constant due to its tiny variation within 10%. The initial aspect ratio  $l_0/w_0$  equals the priority ratio  $\delta$  of the two preferential growth directions along the length and width directions.

(2) In the next growth process, the atoms deposited on a seed crystal upper surface and the effective diffusion area  $\pi R^2 \sim \pi \langle \Delta r^2 \rangle$  around it aggregate to the seed crystal and continue to diffuse along the crystal surface until the lowest surface energy is reached. Here  $R$  is the average diffusion displacement.

(3)  $\delta > 1$  (for the case of  $\delta < 1$ , the discussion is similar).

In the first growth stage, let us suppose that the aspect ratio  $l/w$  of the crystal is invariable, i.e.,  $l/w = l_0/w_0 = \delta$ . Both the width  $w$  and length  $l$  of the seed crystal increase gradually until  $w$  reaches its maximum value  $w_1$ . Subsequently, the width of the crystal, i.e.,  $w_1$ , is fixed and the adatoms contribute to the increment of the crystal length  $l$ , which facilitates the one-dimensional crystal growth.

(4)  $\delta = 1$ . In this case, it is suggested that the aspect ratio of the crystal is a constant during the whole growth process, i.e.,  $l/w = l_0/w_0 = 1$ . Finally, a two-dimensional crystal forms.

## 3. Results and discussion

(1) One-dimensional crystal growth model ( $\delta > 1$ ).

According to the above model, the one-dimensional crystals on the isotropic and quasi-free sustained substrates may go through four growth stages ideally.

Stage I:  $w_0 \leq w < w_1$ ,  $\delta w_0 \leq l < \delta w_1$ .

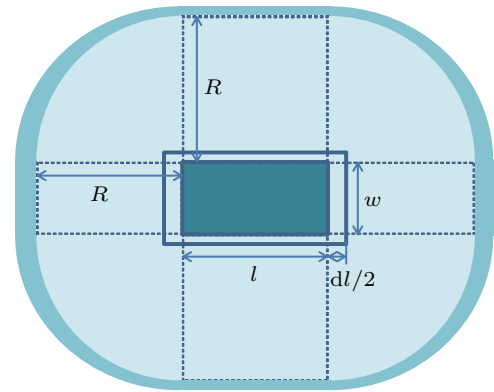


Fig. 1. The schematic illustration of the one-dimensional crystal growth at stage I.

This stage may be considered as a coarsening process of the seed crystal, in which  $l/w = \delta$ . As shown in Fig. 1, the mass supply to the seed crystal coarsening during time interval  $dt$  consists of two parts: (i) the deposition atoms on the seed crystal upper surface and in the tint area around the seed crystal, which is the effective diffusion area, i.e.,  $(lw + 2lR + 2wR + \pi R^2) f dt$ , (ii) the deposition atoms in the ambient dark area, which will be involved in the effective diffusion area with the seed crystal coarsening during time interval  $dt$ , i.e.,  $[(2R + w) dl + (2R + l) dw] ft$ . During this process, the seed crystal extends  $(ldw + wdl) h$ . According to the law of conservation of mass, one can have the following equation:

$$(lw + 2lR + 2wR + \pi R^2) f dt + [(2R + w) dl + (2R + l) dw] ft = (ldw + wdl) h. \quad (1)$$

Due to  $l/w = \delta$  at stage I, equation (1) can be written as

$$\frac{dw}{dt} + \frac{[\delta w^2 + 2(\delta + 1)Rw + \pi R^2] f}{(2\delta w + 2\delta R + 2R) ft - 2\delta hw} = 0. \quad (2)$$

For convenience, equation (2) is rewritten as

$$\frac{dt}{dw} + \frac{2\delta w + 2\delta R + 2R}{\delta w^2 + 2(\delta + 1)Rw + \pi R^2} t = \frac{2\delta hw}{[\delta w^2 + 2(\delta + 1)Rw + \pi R^2]f}. \quad (3)$$

From Eq. (3), one obtains

$$t = \frac{\frac{\delta h}{f} w^2 + C_1}{\delta w^2 + 2(\delta + 1)Rw + \pi R^2}. \quad (4)$$

Using Eq. (4) under the initial condition of  $w(0) = w_0$ , we find  $C_1 = -\frac{\delta h}{f} w_0^2$ , and inserting Eq. (4) yields

$$t = \frac{\frac{\delta h}{f} (w^2 - w_0^2)}{\delta w^2 + 2(\delta + 1)Rw + \pi R^2}. \quad (5)$$

Rearrangement of formula (5) yields

$$w = \frac{(\delta + 1)Rt}{\delta(\frac{h}{f} - t)} + \left\{ \left[ \frac{(\delta + 1)Rt}{\delta(\frac{h}{f} - t)} \right]^2 + \frac{\pi R^2 t + \frac{\delta h}{f} w_0^2}{\delta(\frac{h}{f} - t)} \right\}^{1/2}. \quad (6)$$

Thus, the corresponding length  $l$  is

$$l = \frac{(\delta + 1)Rt}{\frac{h}{f} - t} + \left\{ \left[ \frac{(\delta + 1)Rt}{\frac{h}{f} - t} \right]^2 + \frac{\delta \pi R^2 t + \frac{\delta^2 h}{f} w_0^2}{\frac{h}{f} - t} \right\}^{1/2}. \quad (7)$$

The previous research<sup>[19]</sup> showed that the diffusion coefficient  $D$  of metallic atoms on the silicone oil surface is of the order of  $10^{-11}$  cm<sup>2</sup>/s. Therefore,  $R$  is nearly 100 nm. The Zn crystals exhibit the hexagonal close-packed crystal structure with two main preferential growth directions, i.e., the [0001] and [01 $\bar{1}$ 0] directions.<sup>[18,24]</sup> The priority ratio  $\delta$  should be approximately equal to the average aspect ratio of the crystals. The Zn nanocrystals prepared under the conditions of the deposition rate  $f = 0.01$  nm/s and the film thickness  $H = 8.0$  nm possess an average aspect ratio of 12.<sup>[13]</sup> In this case, it is suggested that  $\delta = 12$ . Moreover, let us suppose that the initial size of the seed crystal is  $w_0 = 1$  nm and  $h = 24$  nm.

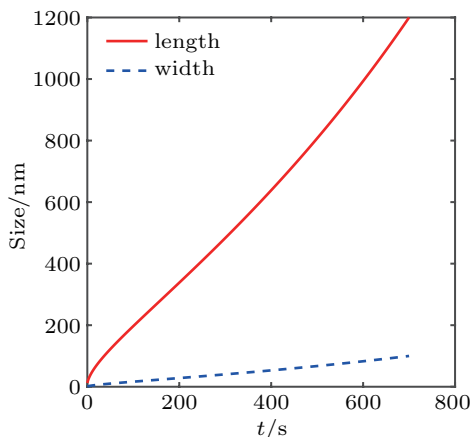


Fig. 2. The growth behaviors of the length and width of the one-dimensional Zn nanocrystals with time at stage I for  $\delta = 12$ .

According to expressions (6) and (7), the dependence of the length  $l$  and width  $w$  of the one-dimensional Zn nanocrystals on time  $t$  at stage I are plotted on Fig. 2. As a whole, both the length  $l$  and width  $w$  of the seed crystal increase gradually with time  $t$  during the coarsening process, as shown in Fig. 2. In the initial phase, the length  $l$  and the width  $w$  increase in velocities of about 7.1 and 0.6 nm/s, respectively. Subsequently, their growth velocities slow down to nearly uniform values of 2.0 and 0.2 nm/s, respectively.

Stage II:  $w = w_1$ ,  $\delta w_1 \leq l < 2\lambda$ .

It can be seen that the growth velocity of the width  $w$  has dropped to 0.2 nm/s at the end of stage I. Additionally, in the case of the deposition rate  $f = 0.01$  nm/s and the film thickness  $H = 8.0$  nm, the width statistical distribution of the as-grown one-dimensional Zn nanocrystals on the silicone oil surface is well fitted by the lognormal distribution, and most of them are less than 100 nm in width.<sup>[12]</sup> Therefore, there seems to be a maximum width  $w_1 = 100$  nm. After that, the width is fixed and all the adatoms are used for the length increment, i.e., stage II.

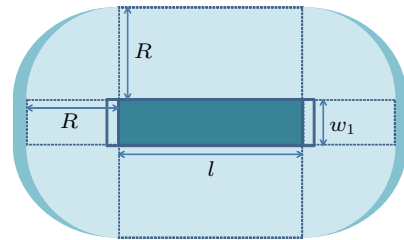


Fig. 3. The schematic illustration of the one-dimensional crystal growth at stage II.

At stage II, as shown in Fig. 3, the mass supply to the length growth during time interval  $dt$  consists of two parts: (i) the deposition atoms on the crystal upper surface and in the tint effective diffusion area around the crystal, i.e.,  $(lw_1 + 2lR + 2w_1R + \pi R^2) f dt$ , (ii) the deposition atoms in the ambient dark area which will be involved in the effective diffusion area with the length increment during time interval  $dt$ , i.e.,  $(w_1 + 2R) f t dl$ . During this process, the crystal extends  $w_1 h dl$ . Therefore, based on the conservation of mass, we obtain the following equation:

$$(lw_1 + 2lR + 2w_1R + \pi R^2) f dt + (w_1 + 2R) f t dl = w_1 h dl, \quad (8)$$

which can be written as

$$\frac{dl}{dt} + \frac{(w_1 + 2R) f}{(w_1 + 2R) f t - w_1 h} l = -\frac{(2w_1R + \pi R^2) f}{(w_1 + 2R) f t - w_1 h}. \quad (9)$$

The general solution to Eq. (9) is given by

$$l = \frac{C_2 - (2w_1R + \pi R^2) f t}{(w_1 + 2R) f t - w_1 h}. \quad (10)$$

Using expression (5) for  $w = w_1$  yields

$$t = \frac{\frac{\delta h}{f} (w_1^2 - w_0^2)}{\delta w_1^2 + 2(\delta + 1)Rw_1 + \pi R^2}.$$

Inserting this boundary condition to expression (10), one obtains  $C_2 = -\delta h w_0^2$ . Thus expression (10) can be written as

$$l = \frac{\left(\frac{\delta w_0^2}{w_1} + w_2\right) t_2}{t_2 - t} - w_2, \quad (11)$$

where  $t_2 = \frac{w_1 h}{(w_1 + 2R)f}$  and  $w_2 = \frac{2w_1 R + \pi R^2}{w_1 + 2R}$ .

According to expression (11), the relationship of the length  $l$  of the one-dimensional Zn nanocrystals with time  $t$  at stage II is depicted in Fig. 4. At the beginning of stage II, the nearly uniform velocity growth of the one-dimensional Zn nanocrystals at the end of stage I continues. Then the one-dimensional Zn nanocrystals will suffer an accelerated growth period for the following reasons. On the one hand, the width  $w$  will not increase anymore and all the adatoms are used for the length growth. On the other hand, the Zn atoms in the ambient dark area accumulate gradually with time  $t$ . At the end of stage II, the length  $l$  of the one-dimensional Zn nanocrystals will reach  $2\lambda$ , where  $\lambda$  is the effective diffusion length on the crystal surface.<sup>[25]</sup>

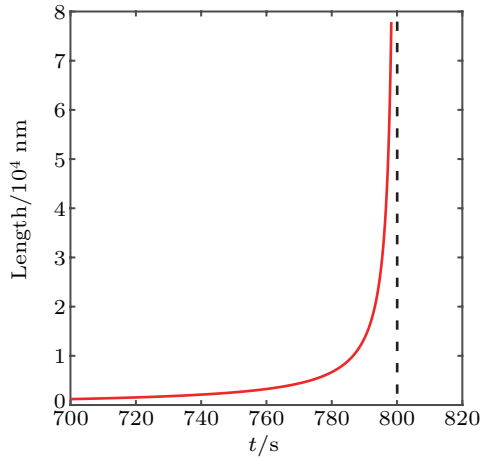


Fig. 4. The relationship of the length of the one-dimensional Zn nanocrystals with time at stage II.

Stage III:  $w = w_1, l \geq 2\lambda, t < H/f$ .

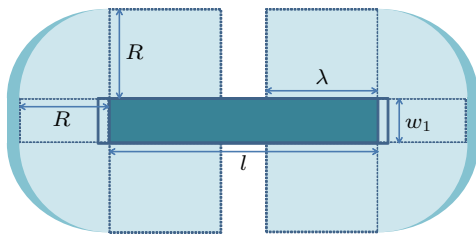


Fig. 5. The schematic illustration of the one-dimensional crystal growth at stage III.

When  $l \geq 2\lambda$ , part of the deposition atoms on the upper and side surface of the one-dimensional crystal will have no chance to move to the emerging tips, as shown in Fig. 5. Therefore, at stage III, the mass supply to the length growth during time interval  $dt$  consists of the following two parts: (i)

the deposition atoms on the crystal upper surface within the effective diffusion length and in the tint effective diffusion areas, i.e.,  $(2\lambda w_1 + 4\lambda R + 2w_1 R + \pi R^2) f dt$ , (ii) the deposition atoms in the ambient dark area, which will be involved in the effective diffusion area with the length increment during time interval  $dt$ , i.e.,  $(w_1 + 2R) f t dl$ . During this process, the crystal extends  $w_1 h dl$ . Therefore, we obtain the following mass conservation equation:

$$\begin{aligned} & (2\lambda w_1 + 4\lambda R + 2w_1 R + \pi R^2) f dt \\ & + (w_1 + 2R) f t dl = w_1 h dl, \end{aligned} \quad (12)$$

which can be written as

$$\frac{dl}{dt} + \frac{(2\lambda w_1 + 4\lambda R + 2w_1 R + \pi R^2) f}{(w_1 + 2R) f t - w_1 h} = 0. \quad (13)$$

Equation (13) possesses the general solution

$$\begin{aligned} l = & -\frac{2\lambda w_1 + 4\lambda R + 2w_1 R + \pi R^2}{w_1 + 2R} \\ & \times \ln [w_1 h - (w_1 + 2R) f t] + C_3. \end{aligned} \quad (14)$$

Using  $l = 2\lambda$  for expression (11) yields

$$t = \frac{2\lambda w_1 h - \delta h w_0^2}{(2\lambda w_1 + 4\lambda R + 2w_1 R + \pi R^2) f}.$$

Based on this boundary condition, one can find

$$\begin{aligned} C_3 = & 2\lambda + \frac{2\lambda w_1 + 4\lambda R + 2w_1 R + \pi R^2}{w_1 + 2R} \\ & \times \ln \frac{2R w_1^2 h + \pi R^2 w_1 h + \delta h w_0^2 w_1 + 2R \delta h w_0^2}{2\lambda w_1 + 4\lambda R + 2w_1 R + \pi R^2} \end{aligned}$$

and inserting the result to expression (14) yields

$$l = (2\lambda + w_3) \ln \frac{\left(\frac{\delta w_0^2}{w_1} + w_3\right) t_3}{(t_3 - t)(2\lambda + w_3)} + 2\lambda, \quad (15)$$

where  $t_3 = t_2 = \frac{w_1 h}{(w_1 + 2R)f}$  and  $w_3 = w_2 = \frac{2w_1 R + \pi R^2}{w_1 + 2R}$ .

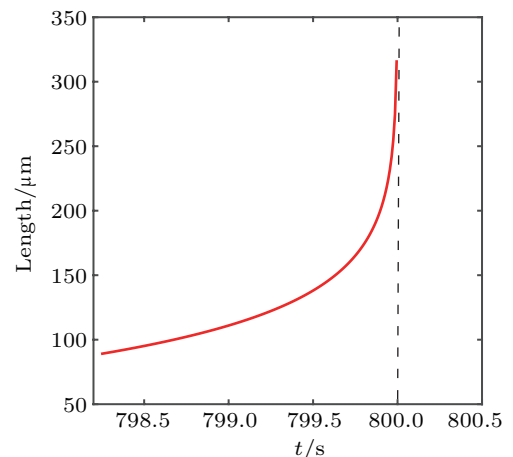


Fig. 6. The dependence of the length of the one-dimensional Zn nanocrystals on time at stage III.

Previous study<sup>[25]</sup> showed that the effective diffusion length  $\lambda$  of the Zn atoms on the Zn crystal surface is about 39  $\mu\text{m}$ . The dependence between the length  $l$  of the one-dimensional Zn nanocrystals and time  $t$  given by expression (15) is drawn in Fig. 6. The atoms from part (i) are constant during time interval  $dt$  at stage III. However, the accumulated atoms from part (ii) are more and more with time  $t$ . Therefore, the growth velocity of the length  $l$  of the one-dimensional Zn nanocrystals will become faster and faster, as shown in Fig. 6.

Stage IV:  $w = w_1, t \geq H/f$ .

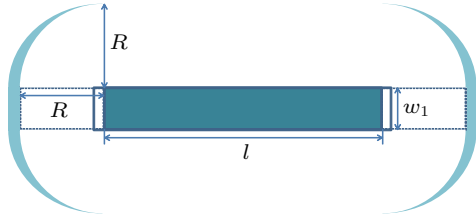


Fig. 7. The schematic illustration of the one-dimensional crystal growth at stage IV.

After deposition ( $t \geq H/f$ ), the mass supply to the length growth during time interval  $dt$  comes from the previous accumulated deposition atoms in the ambient dark area, which will be involved in the effective diffusion area with the length increment, i.e.,  $(w_1 + 2R)Hdl$ . During this process, the crystal extends  $w_1hdl$ . Therefore, one finds the following mass conservation equation:

$$(w_1 + 2R)Hdl = w_1hdl, \quad (16)$$

with the solution

$$w_1 = \frac{2RH}{h - H}. \quad (17)$$

According to expression (17),  $w_1$  is inversely proportional to  $h$ . The morphologies of the one-dimensional crystals are closely related with  $w_1$  and  $h$ , i.e., the one-dimensional crystals exhibit belt-like structure for  $w_1 \gg h$ , while they tend to form crystal rods or wires for  $w_1 \approx h$ . As a result, various morphologies of the one-dimensional crystals can be obtained, which is consistent with our experimental results.<sup>[13]</sup>

When  $w_1 = h$ , expression (17) is similar to the previous computer simulation model,<sup>[26]</sup> i.e.,  $a_0l\Delta L = W^2\Delta L$ , where  $a_0 \sim H$  and  $l \sim (2R + w)$ . The simulation model gives a good explanation of the one-dimensional growth phenomenon of the crystals with the preferential growth direction characteristics. However, it is failed to reveal the detailed growth process of the one-dimensional crystals on the isotropic and quasi-free sustained substrate, such as the dependence of the length  $l$  and width  $w$  on time  $t$ .

In our experiments,<sup>[12]</sup> the most probable length range of the one-dimensional Zn nanocrystals is 250–500 nm for  $f = 0.01$  nm/s and  $H = 8.0$  nm. In this case, most of them are

shorter than 1500 nm and one of the longest one-dimensional Zn nanocrystals is 3.132  $\mu\text{m}$ . According to our model prediction, the one-dimensional Zn nanocrystals may reach 1200 nm and 78  $\mu\text{m}$  at the end of stages I and II, respectively. Therefore, most of the one-dimensional Zn nanocrystals in our experiments are at stage I and only a few can arrive at stage II. Actually, the nucleation density plays an important role in the mass supply for the crystal growth, i.e., it may lead to the absorbing areas around the crystals or seed crystals overlapping or meeting the edges of the substrate.<sup>[26]</sup> Obviously, the larger the nucleation density is, the smaller the average effective absorbing area for every crystal or seed crystal is, i.e., the shorter the average length of the crystals is. The quantitative relationship between the nucleation density and the average length of the crystals is systematically discussed in our previous study.<sup>[26]</sup>

(2) Two-dimensional crystal growth model ( $\delta = 1$ ).

According to the model described above, the aspect ratio  $l/w$  of the crystal is equal to  $\delta$  during the whole growth process in the case of  $\delta = 1$ . As a result, a two-dimensional crystal forms in a two-stage growth process, as shown in Figs. 8 and 10.

Stage I:  $t < H/f$ .

In analogy with the stage I of the one-dimensional crystal growth, using  $\delta = 1$  for expressions (6) and (7) yields

$$l = w = \frac{2Rt}{\frac{h}{f} - t} + \left\{ \left[ \frac{2Rt}{\frac{h}{f} - t} \right]^2 + \frac{\pi R^2 t + \frac{h}{f} w_0^2}{\frac{h}{f} - t} \right\}^{1/2}, \quad (18)$$

which describes the dependence of the length  $l$  and width  $w$  of the two-dimensional crystal on time  $t$  at stage I.

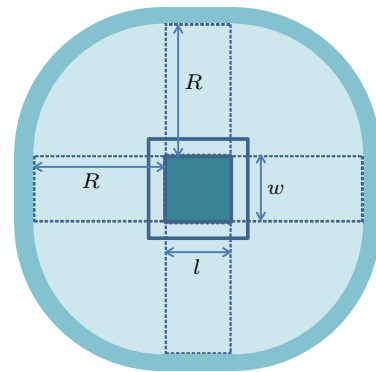
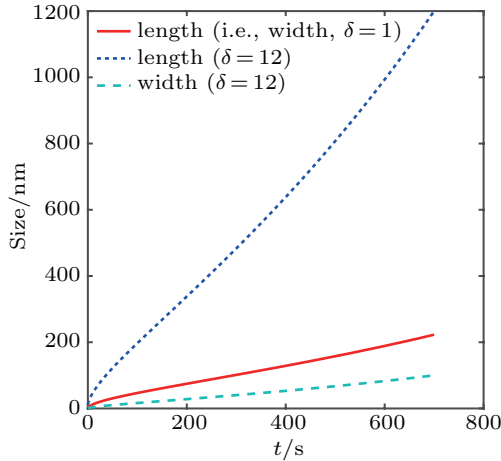


Fig. 8. The schematic illustration of the two-dimensional crystal growth at stage I.

The dependence of the length and width of the two-dimensional Zn nanocrystals on time at stage I for  $\delta = 1$  is depicted in Fig. 9, where the growth behaviors of the one-dimensional Zn nanocrystals with time at stage I for  $\delta = 12$  are supplied for comparison. As shown in Fig. 9, the length (i.e., width) of the two-dimensional Zn nanocrystals possesses a growth velocity of 6.4 nm/s first, and then suffers a slowing growth until a nearly uniform velocity (0.3 nm/s), which is

similar with the growth characteristics of the length and width of the one-dimensional Zn nanocrystals. However, the growth velocity of the length of the two-dimensional Zn nanocrystals is between the length and width growth velocities of the one-dimensional Zn nanocrystals.



**Fig. 9.** The dependence of the length and width of the two-dimensional Zn nanocrystals on time at stage I for  $\delta = 1$  in comparison with the growth behaviors of the one-dimensional Zn nanocrystals with time at stage I for  $\delta = 12$ .

Stage II:  $t \geq H/f$ .

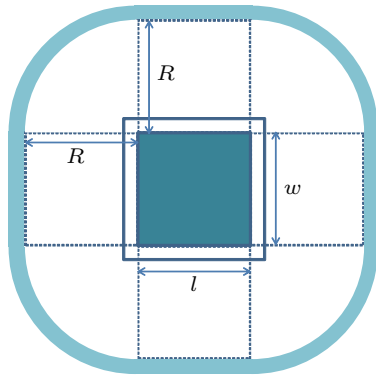


**Fig. 10.** The schematic illustration of the two-dimensional crystal growth at stage II.

After deposition ( $t \geq H/f$ ), the two-dimensional crystal extends  $2hldl$  during time interval  $dt$  by aggregating the previous accumulated deposition atoms in the ambient dark area, i.e.,  $2H(2R+l)dl$ , as shown in Fig. 10. Therefore, we obtain the following mass conservation equation:

$$2H(2R+l)dl = 2hldl \quad (19)$$

with the solution

$$l = \frac{2RH}{h-H}. \quad (20)$$

Expression (20) is similar with expression (17). Analogously,  $l$ , i.e.,  $w$  in the case of  $\delta = 1$ , is inversely proportional to  $h$ , and their relative size plays an important part in the morphologies of the two-dimensional crystals.

The two-dimensional Zn nanocrystals in our experiments include various nanoplates with quadrangular, pentagonal and hexagonal morphologies.<sup>[13]</sup> In our model, for simplicity, the quadrangular nanoplate is selected as a representative sample to reveal the growth characteristics of the two-dimensional Zn nanocrystals on the silicone oil surface. Actually, the value of  $\delta$  is closely related to the morphologies of the seed crystals. Therefore,  $\delta = 1$  is not the only case for the two-dimensional crystal growth on the isotropic and quasi-free sustained substrate, or rather, those priority ratios which are close to  $\delta = 1$  may count. In addition, the crystals may diffuse and rotate on the isotropic and quasi-free sustained substrate during the growth process, which leads an unequal mass supply on various growth directions with the similar priority ratio. These aspects may be responsible for the morphology diversity of the two-dimensional Zn nanocrystals.

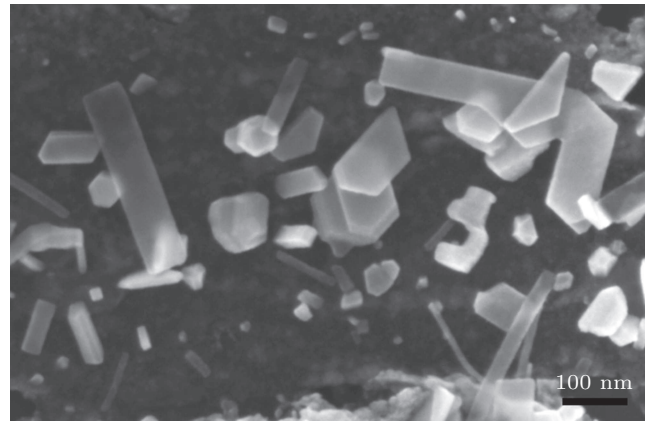


**Fig. 11.** The scanning electron microscope (SEM) image of the low-dimensional Zn nanocrystals on the silicone oil surface ( $f = 0.10$  nm/s,  $H = 8.0$  nm).

In our experiments, the one- and two-dimensional Zn nanocrystals are observed on the silicone oil surface simultaneously, as shown in Fig. 11. According to the statistical result, the priority ratio  $\delta$  of the preferential growth directions of the Zn crystals is of the order of  $10^0 - 10^1$ , which is not quite prominent.<sup>[13]</sup> The competitive growth among the preferential growth directions of the Zn crystals on the silicone oil surface results in the formation of various crystal morphologies.

#### 4. Conclusion

In summary, a new low-dimensional crystal growth model is established on the isotropic and quasi-free sustained substrate. The driven mechanism of the model is based on the competitive growth among the preferential growth directions of the crystals with anisotropic crystal structures, which is different from the conventional VS and VLS mechanism. The model gives a good explanation of the growth kinetics of the low-dimensional Zn nanocrystals on the silicone oil surface, i.e., the dependence of the length and width of the one- and two-dimensional Zn nanocrystals on time. Furthermore, the

model may be useful to reveal the growth mechanism of various low-dimensional crystals fabricated on the liquid substrates, such as perylene,<sup>[27]</sup> graphene,<sup>[10,28–30]</sup> and hexagonal boron nitride.<sup>[31,32]</sup>

In addition, by means of the intrinsic anisotropic crystal structures, many low-dimensional crystals have also been prepared in the liquid environment.<sup>[33–35]</sup> By further considering the competitive growth in  $h$  direction and the mass supply in three-dimensional space, our model may also account for the growth mechanism of various low-dimensional crystals in the isotropic substrates.

## Acknowledgement

We thank Dr. Ziran Ye and Professor Baoxing Li for useful discussions.

## References

- [1] Xu H J, Mi J S, Li Y, Zhang B, Cong R D, Fu G S and Yu W 2017 *Chin. Phys. B* **26** 128102
- [2] Pan Z W, Dai Z R and Wang Z L 2001 *Science* **291** 1947
- [3] Roder H, Hahn E, Brune H, Bucher J P and Kern K 1993 *Nature* **366** 141
- [4] Li Y, Ling H, Gao L, Song Y L, Tian M L and Zhou F Q 2015 *Chin. Phys. Lett.* **32** 107802
- [5] Liu C Y, Miao L, Wang X Y, Wu S H, Zheng Y Y, Deng Z Y, Chen Y L, Wang G W and Zhou X Y 2018 *Chin. Phys. B* **27** 047211
- [6] Wang Z L and Song J H 2006 *Science* **312** 242
- [7] Wagner R S and Ellis W C 1964 *Appl. Phys. Lett.* **4** 89
- [8] Xia Y N, Yang P D, Sun Y G, Wu Y Y, Mayers B, Gates B, Yin Y D, Kim F and Yan H Q 2003 *Adv. Mater.* **15** 353
- [9] Michely T, Hohage M, Bott M and Comsa G 1993 *Phys. Rev. Lett.* **70** 3943
- [10] Geng D C, Meng L, Chen B Y, Gao E L, Yan W, Yan H, Luo B R, Xu J, Wang H P, Mao Z P, Xu Z P, He L, Zhang Z Y, Peng L M and Yu G 2014 *Adv. Mater.* **26** 6423
- [11] Persson A I, Larsson M W, Stenström S, Ohlsson B J, Samuelson L and Wallenberg L R 2004 *Nat. Mater.* **3** 677
- [12] Lu C X, Cheng Y, Pan Q F, Tao X M, Yang B and Ye G X 2016 *Sci. Rep.* **6** 19870
- [13] Lu C X, Jin Y, Tao X M, Yang B and Ye G X 2018 *CrystEngComm* **20** 122
- [14] Gibbs J W 1928 *On the Equilibrium of Heterogeneous Substances* (New York: Longmans)
- [15] Donnay J D H and Harker D 1937 *Am. Mineral.* **22** 446
- [16] Wang H, Song X P, You L and Zhang B 2015 *Scr. Mater.* **108** 68
- [17] Köhl D, Luysberg M and Wuttig M 2010 *J. Phys. D: Appl. Phys.* **43** 205301
- [18] Wang Q, Chen G and Zhou N 2009 *Nanotechnology* **20** 085602
- [19] Ye G X, Michely T, Weidenhof V, Friedrich I and Wuttig M 1998 *Phys. Rev. Lett.* **81** 622
- [20] Luo M B, Ye G X, Xia A G, Jin J S, Yang B and Xu J M 1999 *Phys. Rev. B* **59** 3218
- [21] Einstein A 1905 *Ann. Phys.* **322** 549
- [22] Einstein A 1906 *Ann. Phys.* **324** 371
- [23] Levine I N 1988 *Physical chemistry* 3rd edn (New York: McGraw-Hill)
- [24] Cho S and Lee K H 2010 *J. Mater. Chem.* **20** 6982
- [25] Kast M, Schroeder P, Hyun Y J and Pongratz P 2007 *Nano Lett.* **7** 2540
- [26] Cheng Y, Lu C X, Yang B, Tao X M, Wang J F and Ye G X 2016 *Phys. Lett. A* **380** 2989
- [27] Liu X D, Kaiser V, Wuttig M and Michely T 2004 *J. Cryst. Growth* **269** 542
- [28] Geng D C, Wu B, Guo Y L, Huang L P, Xue Y Z, Chen J Y, Yu G, Jiang L, Hu W P and Liu Y Q 2012 *Proc. Natl. Acad. Sci. USA* **109** 7992
- [29] Guo H, Chen H, Que Y D, Zheng Q, Zhang Y Y, Bao L H, Huang L, Wang Y L, Du S X and Gao H J 2019 *Chin. Phys. B* **28** 056107
- [30] Zhang X F, Liu Z H, Liu W L, Lu X Y, Li Z J, Yu Q K, Shen D W and Xie X M 2019 *Chin. Phys. B* **28** 086103
- [31] Lee J S, Choi S H, Yun S J, Kim Y I, Boandoh S, Park J H, Shin B G, Ko H, Lee S H, Kim Y M, Lee Y H, Kim K K and Kim S M 2018 *Science* **362** 817
- [32] Mo Z J, Hao Z H, Ping X J, Kong L N, Yang H, Cheng J L, Zhang J K, Jin Y H and Li L 2018 *Chin. Phys. B* **27** 016102
- [33] Takeyama Y, Maruyama S and Matsumoto Y 2011 *Cryst. Growth* **11** 2273
- [34] Voigt M, Dorsfeld S, Volz A and Sokolowski M 2003 *Phys. Rev. Lett.* **91** 026103
- [35] Mayers B and Xia Y N 2002 *J. Mater. Chem.* **12** 1875